Monatshefte für Chemie - Chemical Monthly (2022) 153:171–181
https://doi.org/10.1007/s00706-021-02883-8

ORIGINAL PAPER

Dendritic $Cu(OH)_2$ nanostructures decorated pencil graphite electrode as a highly sensitive and selective impedimetric non-enzymatic glucose sensor in real human serum blood samples

Chahira Boukharouba[1] · Mouna Nacef[1] · Mohamed Lyamine Chelaghmia[1] · Rafiaa Kihal[1] · Widad Drissi[1] · Hassina Fisli[2] · Abed Mohamed Affoune[1] · Maxime Pontié[3]

Received: 12 October 2021 / Accepted: 16 December 2021 / Published online: 5 January 2022

Abstract

In this study, an effective and low price non-enzymatic electrochemical glucose sensor was easily elaborated through electrodeposition of highly uniform copper dendrites hydroxide onto pencil graphite electrode ($Cu(OH)_2$/PGE). The obtained electrode was investigated by field-emission scanning electron microscopy, atomic force microscopy, energy-dispersive X-ray spectroscopy, X-ray diffraction, and FT-IR characterizations. The electrocatalytic properties of the modified electrode were investigated by cyclic voltammetry, amperometry, and electrochemical impedance spectroscopy techniques, which can be readily applied to determine glucose using the fabricated sensor, as the results after optimization revealed. Furthermore, a single frequency impedance method was applied for glucose determination as an alternative to conventional EIS methods. The fabricated $Cu(OH)_2$/PGE electrode exhibited a selective impedimetric response towards glucose over an exceptional linear range from 0.1 to 12 mM ($R^2 = 0.999$) with a detection limit of 71.8 µM. Finally, $Cu(OH)_2$/PGE was successfully applied to the assay of glucose in blood samples with unknown interferences.

Graphical abstract

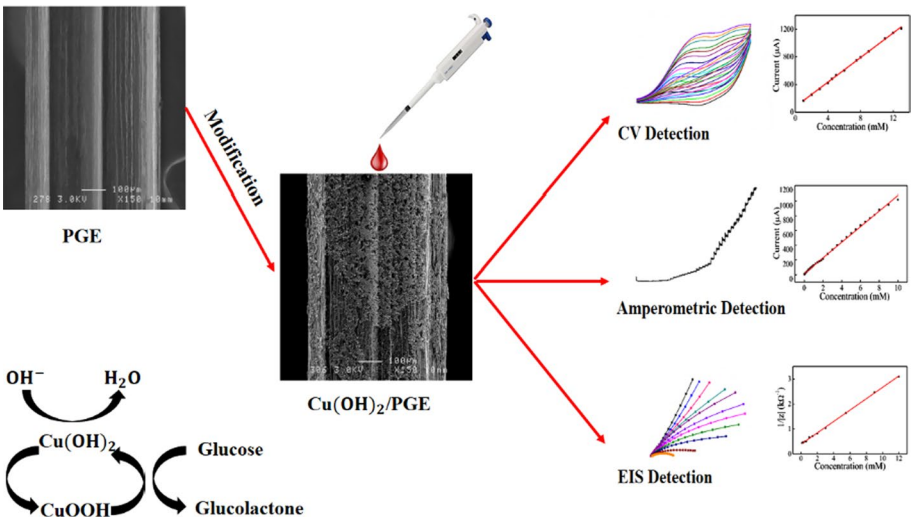

Keywords Copper dendrites · Non-enzymatic glucose sensor · Pencil graphite electrode · Electrochemical impedance spectroscopy

Extended author information available on the last page of the article

Introduction

Recently, many scientists have taken a great interest in the detection of glucose, owing to the importance of its in vivo and in vitro determination in the food industry, pharmaceutical monitoring, and blood [1, 2]. Diabetes is a metabolic chronic disease caused by long-term high blood glucose levels, and often characterized by hyperglycemia. The blood glucose level of diabetic people ranges from 1.1 to 20 mM, while for healthy people it ranges from 3.6 to 7.5 mM. This disease can trigger several major complications, such as heart disease, kidney failure, blindness, nerve disorder, and chronic damage to vessels, etc. [3, 4]. With about 120 million affected people around the world, diabetes has become an incurable pathology that takes the lives of nearly 1 million people yearly [5, 6]. Due to its high impact on human life, there were many efforts conducted to develop accurate, fast, and reliable glucose sensors. Among the methods that were developed to provide an accurate diagnosis and clear data are fluorimetry approaches [7], electrochemiluminescence [8], HPLC [9], Raman spectroscopy [10], infrared spectroscopy [11], capacitive detection [12], and colorimetry [13]. However, the long-term use of these methods added to their high cost constitute an obstacle to their expansive usage.

The electrochemical sensor is considered to be among the most popular and effective glucose detection methods based on the direct catalytic oxidation of glucose, because it is simple, highly sensitive, and has a fast response period [14, 15]. Despite the meritorious features of the enzymatic glucose sensors, such as high sensitivity and selectivity, it still has some intrinsic defects that could reduce the enzymatic activity over time. These defects include difficulties to maintenance circumstances, and lack of long-term stability [16–18].

To address limitations of enzymatic glucose sensors, many researchers have focused on the use of nanostructured electrodes with improved surface area as well as various studies on electrocatalytic activities have been conducted on non-enzymatic glucose sensors [19–23]. The development of these sensors was directed towards the use of several nanomaterials, such as carbon based [24–27], noble metals [28–30], transition metals [31–33], and their oxides [34–38]. Among transition metals, copper-based nanomaterials were the most extensively promising ones due to their exceptional electrochemical properties, low toxicity, low cost, abundance, and an easy preparation. Copper is known for its high electrical conductivity. Hence, a special attention was paid over the last few years, to the development of copper modified electrodes for non-enzymatic glucose sensors [39].

Pencil graphite electrodes (PGEs) possess a lot of advantages like high electrochemical reactivity, market availability, mechanical rigidity, disposable, costless, and could be easily modified [40–43]. Moreover, disposable electrodes, which are used only once, can surpass the regeneration limitations of other solid/hard electrodes. It was stated that PGEs provide a renewal surface that is quicker and more simplified than polishing procedures, common with solid electrodes [44]. In the majority of research reports, PGEs were utilized for the non-enzymatic glucose determination [45–47].

According to a literature review, non-enzymatic amperometric sensors have been widely used for the detection of glucose (Fig. S1). In recent years, electrochemical impedance spectroscopy (EIS) and in particular, the concept of single-frequency analysis was proposed as a transduction principle in the glucose sensors to study the analyte in lower concentrations, to evaluate the interfacial behaviour of electrode [48]. In this technique, at a fixed frequency, the impedance of the electrode/electrolyte interface is measured by AC impedance spectroscopy in low frequency range to establish the relationship between impedance values and glucose concentrations [48–50].

To the best of our knowledge, the use of impedimetric copper hydroxide-modified PGEs for non-enzymatic detection of glucose has not been yet applied in any study. It is with this in mind that a pencil graphite electrode modified by electrochemical deposition of copper hydroxide nanostructures, designated as $Cu(OH)_2$/PGE, is characterized and applied for the high-sensitive amperometric and impedimetric glucose determination in real human blood serum.

Results and discussion

Physical surface characterization

To examine the surface morphologies of unmodified PGE and $Cu(OH)_2$/PGE modified electrodes, field-emission scanning electron microscopy (FE-SEM) and energy-dispersive X-ray spectroscopy (EDX) were recorded in Fig. 1. It can be seen that bare PGE displayed a flat surface and uneven structure (Fig. 1a). After copper electrodeposition, aggregates were densely grown on the PGE surface (Fig. 1b). The aggregates branched and transformed into a three-dimensional copper dendritic microstructure. The Cu dendrites grow in longitudinal and transverse directions, which largely increase the surface area of the material. (Fig. 1c). Figure 1d displays the EDX spectrum of the copper modified PGE, which disclosed a sign for copper, oxygen, sulfur, and carbon ions with an atomic weight of 87.67%, 4.26%, 1.32%, and 6.75%, respectively. The presence of the Cu peak shows the effective modification of Cu on PGE surfaces.

X-ray diffraction patterns of bare PGE and Cu/PGE were also recorded for further examination of the surface

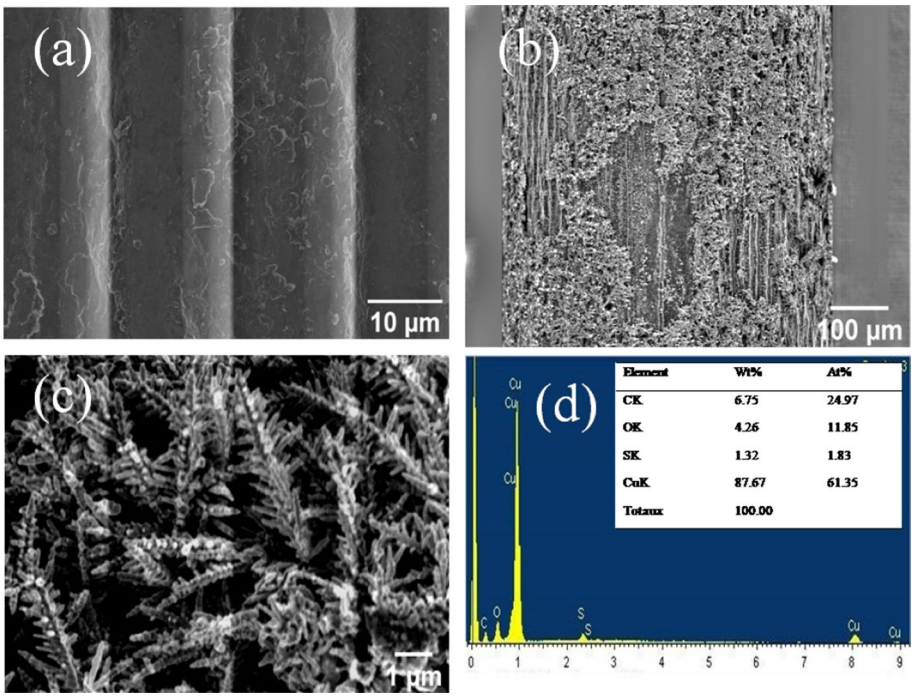

Fig. 1 FE-SEM images of **a** PGE and **b**, **c** $Cu(OH)_2$/PGE at low and high magnification; **d** EDX spectrum of $Cu(OH)_2$/PGE

structure. As shown in Fig. 2a, the peak at angular position 26.75°, corresponds to (002) cubic crystal face structure of graphite carbon. After Cu deposition on PGE surface, the latest diffraction peaks observed at angular positions $2\theta = 43.83°$, 50.77°, and 74.35° were attributed, respectively, to (111), (200), (220) fcc of the Cu structure. FT-IR was employed to further investigate the structure of the prepared materials. As illustrated in Fig. 2b, the FT-IR spectrum of the modified electrode exhibits relevant strong as well as, weaker defined peaks at 3555, 3478, 3413, 1617, 620, and 480 cm^{-1} which were attributed to the free OH group, CuO–H, hydrogen bonded hydroxyl groups, bending mode of the hydroxyl group of water, and Cu–O–H bond, respectively [51–54].

Moreover, atomic force microscopy (AFM) was applied to assess the surface topography of PGE before and after the electrodeposition of copper. Under the 2D and 3D AFM images of PGE and Cu/PGE, as described in Fig. 3a–d, the modified electrode surface had a rough texture, with average roughness of 742 and 856 nm for PGE and Cu/PGE, respectively. Consequently, the large surface area of the modified electrode can provide much more catalytic active sites.

Electrochemical characterization of the copper modified PGE electrode

In this work, cyclic voltammetry (CV) and EIS measurements were used to evaluate the performance of unmodified and modified electrodes in 5 mM $Fe(CN)_6^{3-/4-}$ solution containing 0.1 M KCl (Fig. 4a, b). The CV grams in Fig. 4a display that the potential peak separation between the anodic and cathodic peaks (ΔE_p) was slightly decreased to 120 mV at the modified Cu/PGE compared to 135 mV for unmodified PGE. Moreover, the ratio of the redox peak currents is about 0.96 and 1.42 for unmodified and modified PGE, respectively.

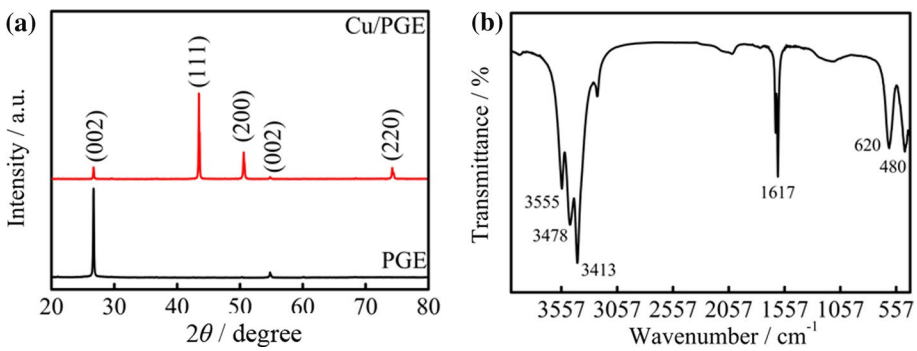

Fig. 2 XRD patterns of unmodified and modified electrodes (**a**); FTIR spectrum of Cu $(OH)_2$/PGE electrode (**b**)

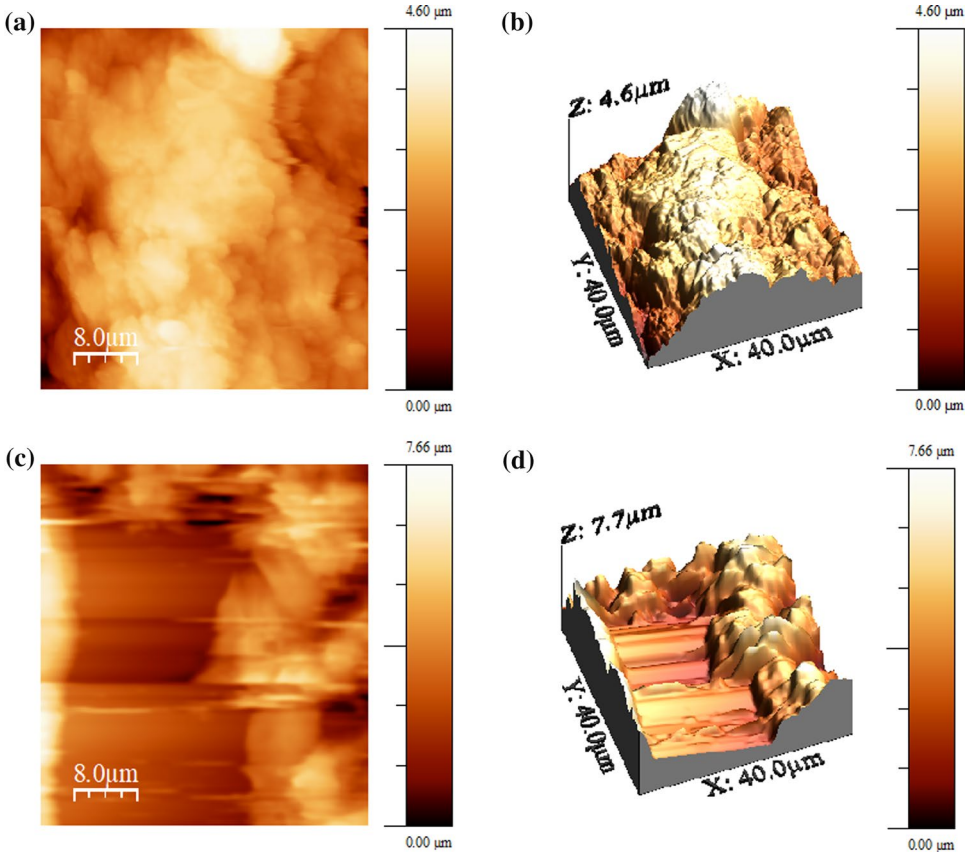

Fig. 3 2D and 3D AFM images of **a**, **b** bare PGE and of **c**, **d** copper modified PGE

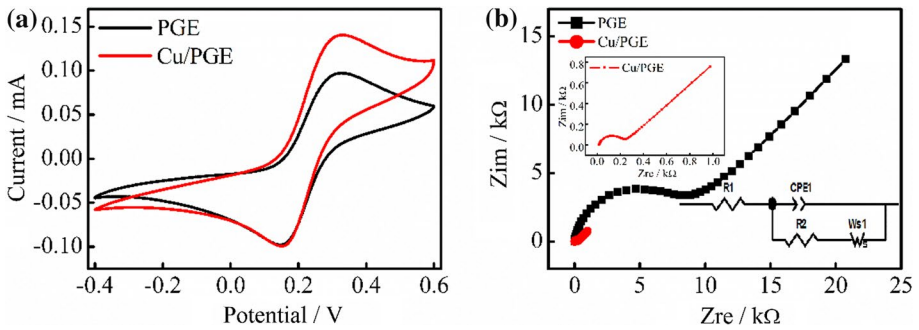

Fig. 4 **a** CV curves and **b** Nyquist plots of the bare PGE and Cu/PGE. The insets show the Nyquist plot of the modified electrode and the equivalent circuit. The supporting electrolyte was 5 mM $Fe(CN)_6^{3-/4-}$ solution containing 0.1 M KCl

The smaller value of ΔE_p and the higher redox peak currents obtained on the modified electrode indicate that the dendrite Cu electrode has high electrical conductivity and better electrochemical properties than the bare PGE electrode, which might be attributed to the 3D structure of dendrite Cu that provided a large surface area, leading to a large electrochemical surface area on the modified electrode.

Figure 4b shows the Nyquist diagram of unmodified and modified electrodes in the same ferricyanide solution (5 mM $Fe(CN)_6^{3-/4-}$ + 0.1 M KCl). EIS was done in the frequency range from 100 kHz to 0.1 Hz at the amplitude voltage of 10 mV. The impedance plots involve two parts; the first one is the semi-circular part which refers to the electron transfer limited process at higher frequencies where the diameter corresponds to the electron transfer resistance (R_2) which refers to the electron transfer process. The second one is the linear portion, which refers to the diffusion process at lower frequencies. The electrical equivalent circuit can describe the faradic impedance of the bare PGE and Cu/PGE. In the Randles equivalent circuit, R_1, CPE_1, R_2, and W_{S1} stand for solution resistance, constant phase element, charge transfer resistance, and Warburg element simulating, respectively (inset Fig. 4b). As illustrated in Fig. 4b, the bare PGE displayed a large semicircle at higher frequencies ($R_2 = 7921\ \Omega$). It can be noticed that the Cu/PGE ($R_2 = 203.8\ \Omega$) is accompanied by a substantial decrease in the interfacial resistance, which indicates that

the PGE surface was successfully covered by copper and that the introduction of copper facilitates the electron transfer. In conclusion, the electrodeposition of the dendrite copper structure on PGE surface area enhanced the electron transfer rate considerably [55, 56].

The electrochemical surface areas of unmodified and modified electrodes were calculated from the slope of anodic peak current I_p versus square root of scan rate $v^{1/2}$ curves (Fig. S2). Randles–Sevcik's equation was used to calculate surface areas, as follows [57, 58]:

$$I_p = 0.436nFAC\sqrt{\frac{nFDv}{RT}} \quad (1)$$

where I_p, C, and D are anodic peak current (A), bulk concentration (mol cm^{-3}), and diffusion coefficient (cm^2 s^{-1}) respectively. The obtained results were 0.07 and 0.10 cm^2 for PGE and Cu/PGE surface areas, respectively (an increase of 30%). Hence, the dendrite Cu structure enhanced the proposed electrode surface area.

Before studying the electrochemical behaviour of the prepared electrode, Cu/PGE was firstly activated by CV in 0.1 M NaOH solution under the potential range from −1.1 to 0.6 V for 15 cycles at 50 mV s^{-1} (Fig. 5). It can be seen that several anodic and cathodic peaks appeared in the cyclic voltammograms of the Cu/PGE electrode, among which the oxidation peaks at −0.412, −0.176, and 0.160 V that indicate the oxidation of Cu(0) to Cu(I), Cu(I) to Cu(II), and Cu(II) to Cu(III), respectively. The reduction peaks at 0.48, −0.56 and −0.86 V are related to the transition of Cu(III) to Cu(II), Cu(II) to Cu(I), and Cu(I) to Cu(0), respectively. Reactions mechanism is respectively as follows [59, 60]:

$$Cu + OH^- \rightarrow CuOH + e^- \quad (2)$$

$$Cu + 2OH^- \rightarrow Cu(OH)_2 + 2e^- \quad (3)$$

$$Cu(OH)_2 \leftrightarrow CuO + H_2O \quad (4)$$

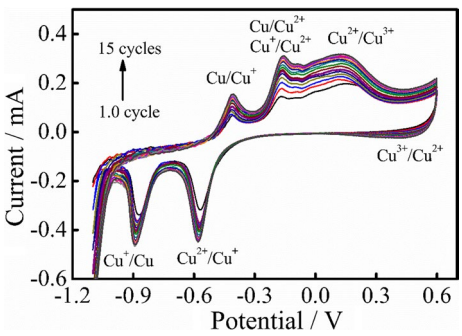

Fig. 5 Cyclic voltammograms of the $Cu(OH)_2$/PGE obtained from an alkaline solution at a scan rate of 50 mV s^{-1} for successive cycling from 1 to 15 cycles

$$CuO + OH^- \leftrightarrow CuOOH + e^- \quad (5)$$

All changes observed in CVs indicate that the formation of copperoxy-hydroxide onto the surface area of PGE was perfectly successful.

Furthermore, the electrochemical behaviour of the $Cu(OH)_2$/PGE was studied by cycling potential from −0.3 to 0.8 V in 0.1 M NaOH solution at various scan rates (Fig. S3a). The redox peak currents increase continuously with the increase of the scan rate from 10 to 1000 mV s^{-1} while the anodic and cathodic peak potentials have a slight positive and negative shifts, respectively. In addition, it can be observed that the oxidation peak current (I_{pa}) and the reduction peak current (I_{pr}) increase linearly with the square root of the scan rate, suggesting a diffusion controlled redox process (Fig. S3b) with the linear regression Eqs. (6) and (7) [61]:

$$I_{pa}/\text{mA} = 0.0271v^{1/2}/(\text{V/s})^{1/2} - 0.1098, R^2 = 0.998 \quad (6)$$

$$I_{pc}/\text{mA} = -0.0255v^{1/2}/(\text{V/s})^{1/2} + 0.0979, \text{R}^2 = 0.998 \quad (7)$$

Electrocatalytic oxidation of glucose

CV and EIS were both performed to explore the electrochemical behaviour of the unmodified and modified electrodes in the absence and the presence of 1.0 mM glucose in 0.1 M NaOH solution at a scan rate of 50 mV s^{-1}. The CVs voltammograms of the unmodified PGE are depicted in the inset of Fig. 6a. It can be seen that no redox peaks appear and there are no changes in current upon adding 1.0 mM glucose in the voltammogram which reflects an insensitivity to glucose which can be explained by the free electrode in metallic impurities.

However, the CVs grams of $Cu(OH)_2$/PGE in 0.1 M NaOH solution in the absence and the presence of 1.0 mM glucose; illustrated in Fig. 6a. No detectable current was observed in the absence of glucose. After the addition of 1.0 mM glucose, the oxidation peak current increased, and the cathodic peak current decreased, indicating the excellent catalytic activity the proposed electrode towards glucose oxidation reaction.

Therefore, the redox couple Cu(II)/Cu(III) is responsible of for the conversion of glucose to glucolactone according to the following reaction [62].

$$CuOOH + \text{glucose} \rightarrow Cu(OH)_2 + e^- + \text{glucolactone} \quad (8)$$

Figure 6b illustrates the Nyquist plots of the proposed electrode $Cu(OH)_2$/PGE prepared under the same conditions as CV. This figure reveals clearly the effect of glucose addition to the alkaline solution in the modification of Nyquist

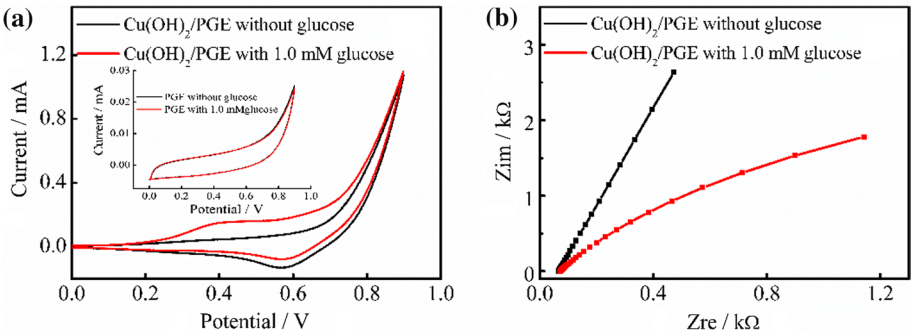

Fig. 6 $Cu(OH)_2$/PGE CVs response (**a**) and Nyquist plots in the absence and presence of 1.0 mM glucose in 0.1 M NaOH solution at 50 mV s^{-1} (**b**). Inset: CVs response of the unmodified in the absence and presence of 1.0 mM glucose in 0.1 M NaOH solution at 50 mV s^{-1}

plots. From a quasi linear curve of sole electrolyte solution, we observe a curved shape when adding glucose (0.1 M), suggesting the decrease in the charge transfer resistance.

This electrocatalytic activity was ascribed to both the excellent catalytic property of $Cu(OH)_2$ and the high surface area provided by the 3D dendrite structure of the electrodeposited Cu. In addition to investigate the effect of different scan rates on the electrocatalytic oxidation behaviour of the prepared electrode, the CV technique was carried out in 0.1 M NaOH aqueous solution with the addition of 1.0 mM glucose at various scan rates (10–1000 mV s^{-1}). Fig. S4a shows that the redox peak currents and peak potentials of the CV curves increase considerably as the scan rates increase, suggesting a quasi-reversible electron transfer reaction. Figure S4b indicates that the redox peak current is linear with the square root of the scan rate according to the following linear regression Eqs. (9) and (10):

$$I_{pa}/\text{mA} = 0.0372v^{1/2}/(\text{V/s})^{1/2} - 0.1048, R^2 = 0.998 \quad (9)$$

$$I_{pc}/\text{mA} = -0.0268v^{1/2}/(\text{V/s})^{1/2} + 0.111, R^2 = 0.994 \quad (10)$$

These outcomes demonstrate that the electrooxidation reaction of glucose was controlled by a typical diffusion-controlled process [63, 64].

To get more information the modified electrode for non-enzymatic glucose sensing application, cyclic voltammetry, amperometry and electrochemical impedance spectroscopy were all used.

Figure 7a illustrates typical CVs curves of the $Cu(OH)_2$/PGE upon successive additions of glucose concentrations from 0.1 to 13 mM in 0.1 NaOH solution. The CVs curves and the Nyquist diagrams of the same electrode for lower and medium glucose concentration are demonstrated in Fig. S5.

It is found that the increase in the glucose concentration is accompanied by an increase in the anodic current, shifting the anodic peak current towards more positive values (see Fig. 7b). Furthermore, peak current densities increased simultaneously with a linear calibration Eq. (11).

$$I_{pa}/\mu\text{A} = 88.926C_{GL}/\text{mM} + 79.24, R^2 = 0.999 \quad (11)$$

The limit of detection (LOD) and the sensitivity of the modified electrode were calculated to be 0.48 µM ($S/N = 3$) and 889.26 µA mM^{-1} cm^{-2}, respectively. Hence, $Cu(OH)_2$/PGE has a remarkable electrocatalytic oxidation impact on glucose detection.

Before analysing the amperometric sensing of glucose on the copper modified electrode, the amperometric response of the $Cu(OH)_2$/PGE upon the successive addition of 0.5 mM of glucose in 0.1 M NaOH solution was recorded at various potentials (see Fig. S6). It has been observed that the response currents rise gradually with the increase of working potential. However, the current intensity from 0.65 to 0.75 V has higher fluctuation, and lower stability than that of 0.55 V, and the higher applied potential could oxidize many interfering species in the blood [56, 61]. So 0.55 V was then chosen as the optimal detection potential.

To determine the sensitivity, the detection limit, and linear range of the proposed sensor, the amperometric glucose detection was realized by consecutive addition of various glucose concentrations from 0.001 to 10 mM, in 0.1 M NaOH solution at the applied potential of 0.55 V and under continuous stirring. As a result, the current response of $Cu(OH)_2$/PGE sensor increased by increasing the glucose concentration (Fig. 7c), providing a linear relationship relying on the two variables. Figure 7d was used to determine the sensitivity and linear range of $Cu(OH)_2$/PGE for glucose detection. The modified glucose sensor shows excellent linearity in the range from 0.001 to 10 mM ($R^2 = 0.998$) with the regression Eq. (12).

$$I_{pa}/\mu\text{A} = 106.465C_{GL}/\text{mM} + 14.063, R^2 = 0.998 \quad (12)$$

The sensitivity was found to be 1064.7 µA mM^{-1} cm^{-2} and the detection limit was 0.2 µM. The Cu II and Cu III redox couple electrocatalytic effect and surface roughness are responsible for increasing the sensitivity of the proposed electrode. Also, the direct growth of $Cu(OH)_2$ on the PGE, without the use of any binder, is considered as significant advantage of the modifying electrode.

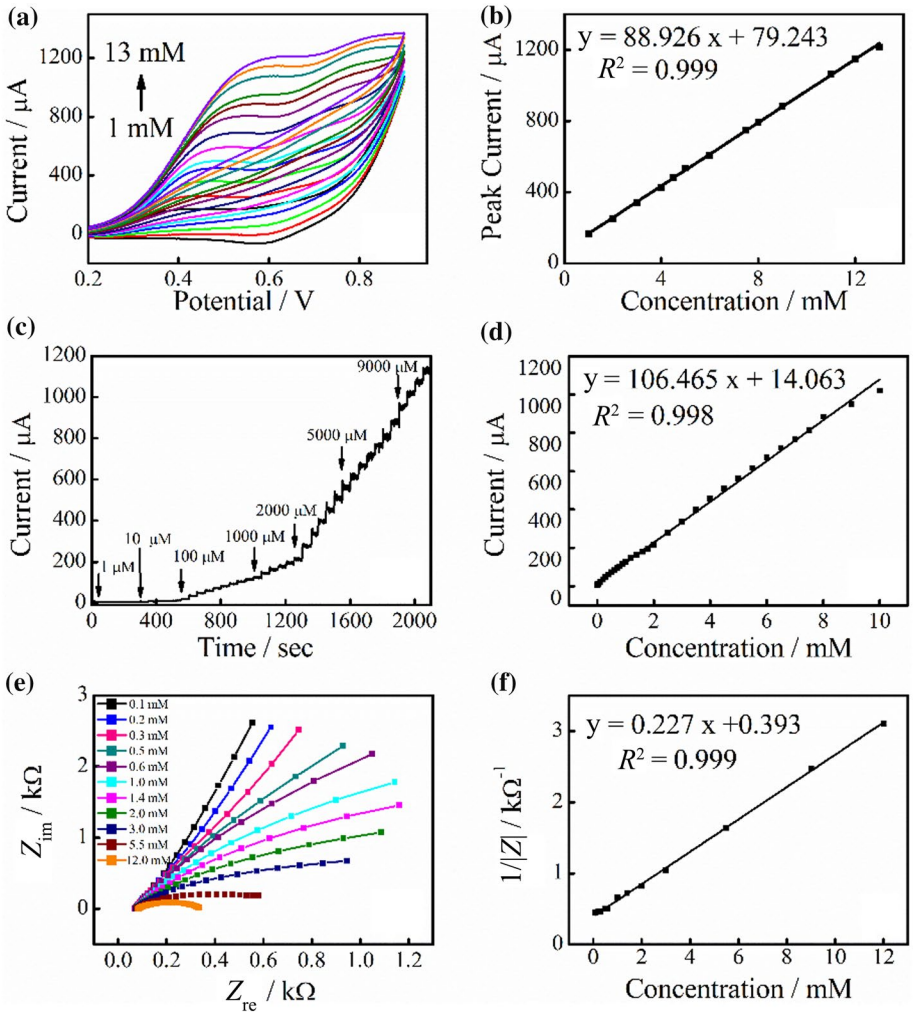

Fig. 7 CV curves (**a**) and corresponding calibration curve (**b**) of modified electrode upon successive additions of glucose (1, 2, 3, 4, 4.5, 5, 6, 7.5, 8, 9, 11, 12, 13 mM) in an alkaline medium. Amperometric response of the same electrode at different glucose concentrations (**c**) and the relationship between the current response and glucose concentration (**d**). Nyquist plots (**e**) and a calibration curve of the $Cu(OH)_2$/PGE (**f**) upon consecutive additions of glucose in an alkaline medium 0.1 M NaOH

Table S1 contains the electrocatalytic performance of $Cu(OH)_2$/PGE electrode and other enzyme-free glucose sensors as mentioned in literature [3, 8, 35, 39, 65–67]. Apart from the observation that the applied potential in this work, is the same or very close to those used in the selected studies, the modified electrode has wider linear range and lower LOD than other copper-based sensors. Also, the sensitivity of the $Cu(OH)_2$ glucose sensor is much higher than most of these nanostructured sensors cited in the Table S1.

As the third method applied here, the analytical response of the glucose sensor was evaluated by the EIS technique. Figure 7e shows the Nyquist diagrams of $Cu(OH)_2$/PGE for selected glucose concentrations to alleviate the figure. The whole curves related to each glucose concentration are gathered in Fig. S4. As stated above, glucose incorporation into sodium hydroxide solution makes a significant change in the Nyquist plot. Furthermore, it can be seen from higher glucose concentrations, that Z_{im} versus Z_{re} graph is depicted by a depressed semicircle in the low frequency zone. When glucose concentration increases from 0.1 to 12 mM in the alkaline solutions, the semicircles diameter decreases gradually, which support that the charge transfer resistance declines [48–50].

A single-frequency impedance is suggested to evaluate the performance of the obtained electrode at 0.125 Hz. Figure 7f illustrates the calibration curve of 1/|Z| vs. glucose concentrations. The linear calibration curve was obtained for $Cu(OH)_2$/PGE electrode in the concentration range of 0.1–12 mM ($R^2 = 0.999$). The limit of detection and the sensitivity were calculated to be 0.227 $k\Omega^{-1}$ mM^{-1} and 71.8 µM, respectively. Compared with other reported research (Table 1), as an obtained electrode which is used as a new impedimetric sensor, shows higher sensibility, a lower limit of detection and a wider linear range.

The comparison of the obtained results reveals that EIS gives a wider linear range for glucose determination. Nevertheless, the amperometric technique provides the highest sensitivity and the lower limit of detection.

Table 1 The $Cu(OH)_2$/PGE electrode as an impedimetric non-enzymatic glucose sensor in comparison with previous literature reports

Electrode	Sensitivity	Linear range /mM	LOD /μM	Ref
MIP@Ni foam[a]	–	10–55	–	[2]
EAuNi$(OH)_2$[b]	0.484 kΩ/mM	0.1–2	370	[48]
Ni$(OH)_2$/SPE[c]	0.137 $k\Omega^{-1}$/mM	0.1–2	315	[49]
Ni$(OH)_2$/SPE[d]	0.168 $k\Omega^{-1}$/mM	0.1–4	53	[50]
Cu$(OH)_2$/SPE[e]	0.475 $k\Omega^{-1}$/mM	0.2–10	51	[50]
Ni$(OH)_2$/Cu$(OH)_2$/SPE[f]	0.705 $k\Omega^{-1}$/mM	0.1–5	40	[50]
FTO/Nano-NiO/GOx[g]	4.45 kΩ/mM	0.2–4	24	[70]
Ni$(OH)_2$/AuNp/SPE[h]	0.073 $k\Omega^{-1}$/mM	0.1–2	40	[71]
TiO_2/APTES@CG/GOx[i]	–	0.05–1	24	[72]
FTO/Nano-CuO/Chitosan/GOx[j]	0.261 kΩ/mM	0.2–15	27	[73]
Cu$(OH)_2$ /PGE	0.227 $k\Omega^{-1}$/mM	0.1–12	71.8	This work

[a]Molecularly imprinted polymers (MIPs) modified porous Ni foam

[b]Gold electrode modified by thin films of nickel hydroxide

[c]Nickel hydroxide nanoparticles (Ni$(OH)_2$) onto a screen-printed electrode (SPE)

[d]Nickel hydroxide Ni$(OH)_2$ modified screen-printed graphite macroelectrode (SPE)

[e]Copper hydroxide Cu$(OH)_2$ modified screen-printed graphite macroelectrode (SPE)

[f]Copper hydroxide Cu$(OH)_2$ modified screen-printed graphite macroelectrode (SPE),nickel hydroxide Ni$(OH)_2$ modified Cu$(OH)_2$/SPE

[g]Nanostructured nickel oxide (Nano-NiO) modified F-doped SnO_2 conducting glass (FTO) glucose oxidase enzyme (GOx) modified FTO/Nano-NiO

[h]Gold nanoparticles (AuNp) modified screen-printed electrodes (SPE), nickel hydroxide (Ni$(OH)_2$) modified AuNp/SPE

[i]Titanium dioxide(TiO_2) modified with 3-aminopropyltriethoxysilane (APTES) TiO_2/APTES cross-linked with carboxylic graphene (CG) glucose oxidase (GOx) added to TiO_2/APTES@CG

[j]Nanostructured copper oxide (Nano-CuO) sputtered on the fluorinated-tin oxide (FTO) layer glucose oxidase (GOx) was mixed with the chitosan Chitosan/GOx was deposited on FTO/Nano-CuO

Anti-interference and stability of Cu$(OH)_2$/PGE

The anti-interference and stability study were conducted using the amperometric technique. In fact, besides glucose, there are major interfering substances that naturally co-exist in human blood serum, such as uric acid, ascorbic acid, acetaminophen, and sucrose. The concentration of glucose is 30 times higher than that of these substances in human blood serum [68, 69]. The oxidation current obtained from an interfering substance like uric acid, ascorbic acid, acetaminophen, and sucrose, was measured to perform the selectivity analysis. The interference studies were carried out on Cu$(OH)_2$/PGE modified electrode by successive injection of 1.0 mM of glucose, 0.1 mM of AA, 0.1 mM of AP, 0.1 mM of UA, and 0.1 mM of Suc in 0.1 M NaOH solution at 0.55 V. It can be seen in Fig. 8a that the response current of interfering species is very low even negligible when compared with that of glucose. Thus, the Cu$(OH)_2$/PGE electrode has an exceptional selectivity and excellent anti-interference performance.

On the other hand, cyclic voltammetry was used to investigate the prepared sensor stability at various storage periods (21 days) under optimum conditions. From Fig. 8b it is noticed that the current decreases slowly (7%) which

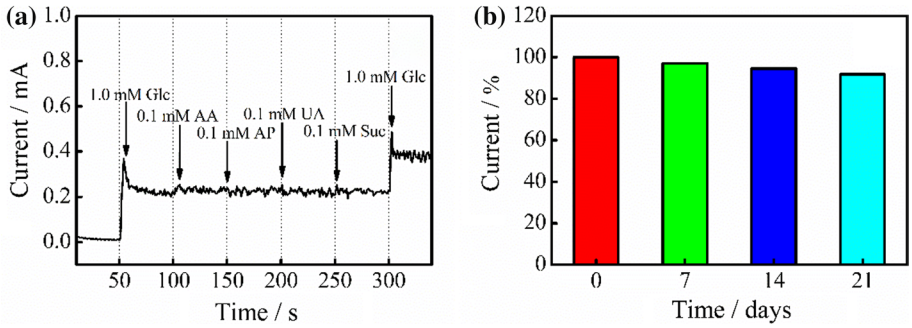

Fig. 8 **a** Current response curves of the modified electrode after injection of 1 mM of glucose and interfering species in alkaline solution at 0.55 V. **b** Stability of the Cu$(OH)_2$/PGE stored under optimum conditions for 21 days using 0.5 mM of glucose in 0.1 M NaOH

demonstrate that the proposed $Cu(OH)_2$/PGE sensor has good stability.

Detection of glucose in human blood serum

To assess the commercial reliability and applicability of the developed electrochemical glucose sensor, the glucose level in the human blood serum samples was analyzed by a commercial glucometer and then by our sensor using impedimetric measurements. As shown in Table 2, the non-enzymatic glucose sensor displays recoveries in the range of 99.24–104.57% showing excellent practicability in the determination of glucose in real serum samples.

Conclusion

A novel dendritic $Cu(OH)_2$/PGE as impedimetric non-enzymatic glucose sensor was successfully elaborated by an effective, low and fast two steps electrochemical method. The glucose sensing application of the proposed electrode was investigated by cyclic voltammetry, amperometry, and electrochemical impedance spectroscopy. The results demonstrate that $Cu(OH)_2$/PGE sensor provides a good level of sensitivity, linear range, and limit of detection. Also, the designed impedimetric $Cu(OH)_2$/PGE was successfully applied to detect glucose in human serum with highly accuracy. For all of these reasons, we believe that obtained sensor can be used as a potential candidate for routine analysis and determination of glucose.

Experimental

All chemicals involved in this work were used without further purification and had an analytical grade. Copper sulfate pentahydrate ($CuSO_4{\cdot}5H_2O$), sodium hydroxide, (NaOH), and sodium sulfate (Na_2SO_4) were obtained from Sigma-Aldrich. While potassium hexacyanoferrate ($K_4Fe(CN)_6$) and ($K_3Fe(CN)_6$), D(+)-glucose, uric acid (UA), L-ascorbic acid (AA), acetaminophen (AP), sucrose (Suc) were procured from Fluka. All solutions were prepared with distilled water (DI). Human serum samples were obtained from the local hospital.

A potentiostat (Versa STAT 3, Princeton Applied Research, AMETEK, USA) was used to perform electrochemical experiments. A three-electrode electrolytic cell was employed for all electrochemical measurements; saturated calomel electrode (SCE) was used as the reference electrode (3.5 M KCl), unmodified and modified electrodes were the working electrode and platinum wire was set as the counter electrode. All potentials were quoted in respect to the SCE electrode. A Rotring pencil (model T, 2B, 0.7 mm diameter) was purchased from Rotring (Germany). The PGE has been prepared by cutting the leads into 6 cm long sticks and 2 mm was dipped in electrolyte, the geometric surface area was calculated and estimated to be 0.047 cm^2.

Atomic force microscopy (AFM) (BRUKER, Germany), field emission scanning electron microscope (FE-SEM) (JEOL, 6301F, Japan) and energy-dispersive X-ray analyzer (EDX) measurements were used to examine the morphological features. X-ray diffraction pattern analysis (XRD) (Bruker D8 Discover spectrometer) and Fourier Transform Infrared (FT-IR) (Perkin Elmer in the wavelength range of 4000 to 500 cm^{-1}) measurements were used to analyse the structure of the proposed sensor.

Preparation of the modified electrode

After subsequent sonication for 2 min in DI, and acetone, bare PGE was kept at room temperature till use. A solution of $CuSO_4{\cdot}5H_2O$ 0.2 M and Na_2SO_4 0.2 M (pH 3.5) was used for electrochemical deposition of copper onto the working electrode to get Cu/PGE. Copper electrodeposition was carried out by applying a potential between −0.3 and −0.5 V at a fixed scan rate of 50 mV s^{-1} for 6 cycles at 45 °C in the above described solution. After that, the prepared electrode was washed, dried in the air. Lastly, the modified electrode was transformed into $Cu(OH)_2$/PGE using multiple scan cyclic voltammetry between − 1.1 V and 0.6 V in an alkaline medium (NaOH, 0.1 M) for15 cycles at 50 mV s^{-1}.

Electrochemical studies

The bare PGE and $Cu(OH)_2$/PGE electrodes were investigated as a glucose sensors in 0.1 M NaOH solution. CV measurements were carried out in the potential range between 0 and 0.9 V, acquired at a fixed scan rate of

Table 2 Determination of glucose in blood serum samples

Samples	Concentration of glucose/mM		Recovery /%	Added glucose / mM	Found glucose / mM	Recovery/%
	This sensor	Determined by a commercial glucometer				
1	4.18	4.13	101.21	2.00	6.11	101.1
2	7.55	7.22	104.57	2.00	9.42	101.3
3	10.49	10.57	99.24	2.00	12.15	102.7

50 mV s^{-1} in alkaline medium. Amperometry measurements at various concentrations of glucose were performed at a potential 0.55 V in the stirred alkaline medium. Electrochemical impedance spectroscopy (EIS) as a highly sensitive and effective technique was used to determine the performance of the fabricated glucose sensor. The working potential was optimized at + 0.35 V and the frequency range was varied from 100 kHz to 0.1 Hz. To investigate $Cu(OH)_2$/PGE sensor, module (|Z|) of complex impedance was analysed at 0.125 Hz. The interference studies were carried out on $Cu(OH)_2$ modified electrode by successive injection of 1 mM of glucose (Glc), 0.1 mM of ascorbic acid (AA), 0.1 mM of acetaminophen (AP), 0.1 mM of uric acid (UA), and 0.1 mM of sucrose (Suc) in 0.1 M NaOH solution at 0.55 V. The amperometric current obtained from an interfering substance was measured to perform the selectivity analysis. Also, the cyclic voltammetry was used to investigate the storage stability of the prepared sensor at various storage periods (21 days). All experiments were run at room temperature except the electrodeposition of copper which was performed at 45 °C.

Supplementary Information The online version contains supplementary material available at https://doi.org/10.1007/s00706-021-02883-8.

Acknowledgements We are very grateful to the financial support within the General Direction of Scientific Research and Technology Development of the Algerian ministry of higher education and scientific research.

References

1. Amirzadeh Z, Javadpour S, Shariat MH, Knibbe R (2018) Synth Met 245:160
2. Li X, Niu XH, Wu HY, Meng SC, Zhang WC, Pan JM, Qiu FX (2017) Electroanalysis 29:1243
3. Vinoth V, Shergilin TD, Asiri AM, Wu JJ, Anandan S (2018) Mater Sci Semicond Process 82:31
4. Liu W, Chai G, Zhao X, Dai Y, Qi Y (2020) Sens Actuators B 321:128485
5. Chen H, Sun P, Qiu M, Jiang M, Zhao J, Han D, Niu L, Cui G (2019) J Electroanal Chem 841:119
6. Huang KJ, Wang L, Li J, Gan T, Liu YM (2013) Measurement 46:378
7. Mai LNT, Tran TH, Bui QB, Nhac-Vu HT (2019) Colloids Surf A 582:123936
8. Zhao Y, Bo X, Guo L (2015) Electrochim Acta 176:1272
9. Zhang S, Li C, Zhou G, Che G, You J, Suo Y (2013) Carbohydr Polym 97:794
10. Barone PW, Parker RS, Strano MS (2005) Anal Chem 77:7556
11. Petibois C, Rigalleau V, Melin AM, Perromat A, Cazorla G, Gin H, Déléris G (1999) Clin Chem 45:1530
12. Cheng Z, Wang E, Yang X (2001) Biosens Bioelectron 16:179
13. Morris NA, Cardosi MF, Birch BJ, Turner APF (1992) Electroanalysis 4:1
14. Ju L, Wu G, Lu B, Li X, Wu H, Liu A (2016) Electroanalysis 28:2543
15. Crapnell RD, Street RJ, Ferreira-Silva V, Down MP, Peeters M, Banks CE (2021) Anal Chem 93:13235
16. Jeong H, Kwac LK, Hong CG, Kim HG (2021) Mater Sci Eng, C 118:111510
17. Esmaeeli A, Ghaffarinejad A, Zahedi A, Vahidi O (2018) Sens Actuators B 266:294
18. Evans RG, Banks CE, Compton RG (2004) Analyst 129:428
19. Zhuang Z, Su X, Yuan H, Sun Q, Xiao D, Choi MMF (2008) Analyst 133:126
20. Tian K, Prestgard M, Tiwari A (2014) Mater Sci Eng C 41:100
21. Zheng W, Li Y, Hu L, Lee LYS (2019) Sens Actuators B 282:187
22. Zheng W, Hu L, Lee LYS, Wong KY (2016) Electroanal Chem 781:155
23. Wang X, Zhang Y, Banks CE, Chen Q, Ji X (2010) Colloids Surf B 78:363
24. Hao L, Li SS, Wang J, Tan Y, Bai L, Liu A (2020) J Electroanal Chem 878:114602
25. FabriceRolandBako Y, Tapsoba I, Pontie M, Chelaghmia ML (2018) Int J Electrochem Sci 13:8056
26. Chelaghmia ML, Nacef M, Fisli H, Affoune AM, Pontié M, Makhlouf A, Derabla T, Khelifi O, Aissat F (2020) RSC Adv 10:36941
27. Chelaghmia ML, Nacef M, Affoune AM (2012) J Appl Electrochem 42:819
28. Cui HF, Ye JS, Zhang WD, Li CM, Luong JHT, Sheu FS (2007) Anal Chim Acta 594:175
29. Ryun J, Kim K, Kim HS, Hahn HT, Lashmore D (2010) Biosens Bioelectron 26:602
30. Cherevko S, Chung CH (2009) Sens Actuators B 142:216
31. Wu HX, Cao WM, Li Y, Liu G, Wen Y, Yang HF, Yang SP (2010) Electrochim Acta 55:3734
32. Tang J, Wei L, He S, Li J, Nan D, Ma L, Shen W, Kang F, Lv R, Huang Z (2021) Materials 14:5067
33. Riman D, Bartosova Z, Halouzka V, Vacek J, Jirovsky D, Hrbac J (2015) RSC Adv 5:31245
34. Yuan G, Yu S, Jie J, Wang C, Li Q, Pang H (2020) Chin Chem Lett 31:1941
35. Luo S, Su F, Liu C, Li J, Liu R, Xiao Y, Li Y, Liu X, Cai Q (2011) Talanta 86:157
36. Yang P, Wang X, Ge C, Fu X, Liu XY, Chai H, Guo X, Yao HC, Zhang YX, Chen K (2019) Appl Surf Sci 494:484
37. Yang YJ, Li W, Chen X (2012) Electrochem 16:2877
38. Li C, Yamahara H, Lee Y, Tabata H, Delaunay JJ (2015) Nanotechnology 26:305503
39. Wei C, Liu Y, Liu Q, Xiang W (2019) Electroanal Chem 835:273
40. Kawde AN, Aziz MA (2014) Electroanalysis 26:2484
41. Majidi MR, Asadpour-Zeynali K, Hafezi B (2009) Electrochim Acta 54:1119
42. Nacef M, Chelaghmia ML, Khelifi O, Pontié M, Djelaibia M, Guerfa R, Bertagna V, Vautrin-Ul C, Fares A, Affoune AM (2021) Int J Hydrogen Energy 46:37670
43. Nacef M, Chelaghmia ML, Affoune AM, Pontié M (2018) Electroanalysis 31:113
44. Oghli AH, Soleymanpour A (2020) Mater Sci Eng C 108:110407
45. Surucu O, Abaci S (2017) Mater Sci Eng C 78:539
46. Kouchakinejad S, Babaee S, Roshani F, Kouchakinejad R, Shirmohammadi N, Kaki S (2020) Chem Phys Lett 759:137987
47. Justice Babu K, Sheet S, Lee YS, Gnana Kumar G (2018) ACS Sustain Chem Eng 6:1909
48. Rinaldi AL, Carballo R (2016) Sens Actuators B 228:43
49. Rinaldi AL, Sobral S, Carballo R (2017) Electroanalysis 29:1961
50. Chelaghmia ML, Fisli H, Nacef M, Brownson DAC, Affoune AM, Satha H, Banks CE (2021) Anal Methods 13:2812
51. Ahmadi F, Ghasemi S (2018) J Mater Sci Mater Electron 29:9067
52. Awwad AM, Albiss B (2015) Adv Mater Lett 6:51

53. Shackery I, Patil U, Pezeshki A, Shinde NM, Kang S, Im S, Jun SC (2016) Electrochim Acta 191:954
54. Momeni S, Farrokhnia M, Karimi S, Nabipour I (2016) J Iran Chem Soc 13:1027
55. Wu H, Yan Y, Huang Q, Liang G, Qiu F, Ye Z, Liu D (2020) New J Chem 44:12723
56. Luo J, Jiang S, Zhang H, Jiang J, Liu X (2012) Anal Chim Acta 709:47
57. Ferrari AGM, Foster CW, Kelly PJ, Brownson DAC, Banks CE (2018) Biosensors 8:53
58. Chelaghmia ML, Nacef M, Affoune AM, Pontié M, Derabla T (2018) Electroanalysis 30:1117
59. Zhang Y, Su L, Manuzzi D, de los Monteros HVE, Jia W, Huo D, Hou C, Lei Y (2012) Biosens Bioelectron 31:426
60. Li J, Tang J, Wei L, He S, Ma L, Shen W, Kang F, Huang Z (2020) New Carbon Mater 35:410
61. Dat PV, Viet NX (2019) Mater Sci Eng C 103:109758
62. Dayakar T, Rao KV, Bikshalu K, Rajendar V, Park SH (2017) J Mater Sci: Mater Med 28:109
63. Siampour H, Abbasian S, Moshaii A (2020) Appl Surf Sci 518:146182
64. Li YY, Kang P, Huang HQ, Liu ZG, Li G, Guo Z, Huang XJ (2020) Sens Actuators B 307:127639
65. Li L, Liu Y, Ai L, Jiang J (2019) J Ind Eng Chem 70:330
66. Song J, Xu L, Zhou C, Xing R, Dai Q, Liu D, Song H (2013) ACS Appl Mater Interfaces 5:12928
67. Pourbeyram S, Mehdizadeh K (2016) J Food Drug Anal 24:894
68. Palve YP, Jha N (2020) Mater Chem Phys 240:122086
69. Rozsypal J, Riman D, Halouzka V, Opletal T, Jirovsky D, Prodromidis M, Hrbac J (2018) J Electroanal Chem 816:45
70. Asrami PN, Tehrani MS, Azar PA, Mozaffari SA (2017) Electroanal Chem 801:258
71. Rinaldi AL, Rodríguez Castellón E, Sobral S, Carballo R (2019) J Electroanal Chem 832:209
72. Ognjanović M, Stanković V, Knežević S, Antić B, Vranješ-Djurić S, Stanković DM (2020) Microchem J 158:105150
73. Naderi Asrami P, Mozaffari SA, Saber Tehrani M, Aberoomand Azar P (2018) Int J Biol Macromol 118:649

Authors and Affiliations

Chahira Boukharouba[1] · Mouna Nacef[1] · Mohamed Lyamine Chelaghmia[1] · Rafiaa Kihal[1] · Widad Drissi[1] · Hassina Fisli[2] · Abed Mohamed Affoune[1] · Maxime Pontié[3]

✉ Mohamed Lyamine Chelaghmia
chelaghmia.mohamedlyamine@univ-guelma.dz;
amine_chelaghmia@yahoo.fr

[1] Laboratoire d'Analyses Industrielles et Génie des Matériaux, Département de Génie des Procédés, Université 8 Mai 1945 Guelma, BP 401, 24000 Guelma, Algeria

[2] Laboratoire de Chimie Appliquée, Département des Sciences de la Matière, Université 8 Mai 1945 Guelma, BP 401, 24000 Guelma, Algeria

[3] Groupe Analyses et Procédés (GA&P), Faculty of Sciences, University of Angers, 2 Bd. Lavoisier, 49045 Angers Cedex 01, France